**Proceedings of the 11th ICPMG 2026**
11th International Conference on Physical Modelling in Geotechnics
8-12 June 2026, Zurich, Switzerland


# Hydraulic Model Experiments of Wave–Soil–Structure Interactions in a Drum Centrifuge

J. Miyamoto, K. Tsurugasaki
*Technical Research Institute, Toyo Construction, Nishinomiya, Japan,*
*miyamoto-junji13@toyo-const.co.jp, tsurugasaki-kazuhiro@toyo-const.co.jp*

**ABSTRACT:** This paper demonstrates the effectiveness of drum-type centrifugal hydraulic model experiments for investigating wave–soil–structure interactions and stability of coastal or offshore structure-foundation systems. While conventional hydraulic flume experiments and beam-type centrifuge tests are limited by scale and domain size, the drum-type centrifuge overcomes these constraints by enabling prototype-scale stresses and expanded spatial domains. Physical modelling and scaling laws were applied to key offshore processes-including seepage flow both in the rubble mound and sand bed under tsunami overflow, pore pressure responses leading to liquefaction during wave loading, and gravity flow dynamics of clay slurries. Three experimental approaches are presented: tsunami overflow tests assessing breakwater resilience and sand transport through the mound induced by seepage flow, wave-induced liquefaction and associated subsidence of submerged rubble mounds, and sediment gravity flow tests under varying water content. Results reveal the effectiveness of breakwater reinforcement, mechanisms of wave-induced liquefaction and foundation sinking, and the effects of clay water content on the characteristics of turbulent slurry flow. Drum-type centrifuge testing thus provides a valuable tool for realistic assessment and design of resilient coastal structures under prototype stress fields.

## 1 INTRODUCTION

The instability of the foundation of coastal or offshore structures has received considerable attention in relation to the action of storm waves, tsunami or other such water motion as well as earthquakes (Figure1). However, the challenges in onsite observations of the dynamic process of instability, such as scouring, erosion and failure, in the foundation under such water motion are formidable in most cases, if not impossible.

Hydraulic model experiments are widely used in coastal engineering to investigate interactions among waves, coastal structures, and seabed soils, typically employing scale models in long flumes under normal gravity ($1g$) conditions. However, these experiments are generally limited to small-scale models because of flume height and width restrictions. In geotechnical engineering, similar studies are less common, but some model tests examining interactions between waves or tsunami and soil or gravels are conducted using centrifuges (Sassa & Sekiguchi, 1999; Takahashi et al., 2014; Takahashi et al., 2024). Conventional beam-type centrifuges, however, limit the size of soil containers, making it difficult to reproduce the wide flume conditions required for modelling large-scale wave and flow phenomena.

To overcome these limitations, we use a drum-type centrifuge apparatus with a cylindrical flume, which allows hydraulic model tests that reproduce not only prototype-scale stress and pressure conditions but also enable investigations of coupled water-soil processes over a larger spatial domain under centrifugal acceleration (Baba et al. 2002; Miyake et al. 2009; Tsurugasaki et al., 2018; Miyamoto et al. 2019). This paper demonstrates that drum-type centrifugal

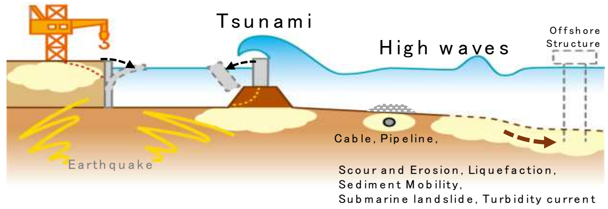


*Figure1. Illustration depicting dynamic problems of water-soil-structure from nearshore to offshore*

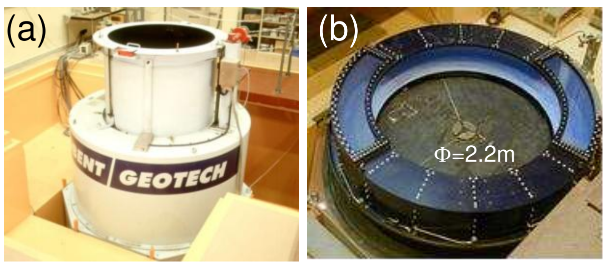


*Figure 2. (a) Exterior view of the drum centrifuge. (b) The cylindrical container installed inside the drum centrifuge.*

hydraulic model experiments make it possible to examine the stability of system in terms of wave–soil–structure interactions.

In this paper, we focus on the physical modelling of key offshore processes depicted in Figure 1, namely tsunami, high waves, and submarine slides. We describe experimental methods and applications using a drum-type centrifuge, including: structural stability evaluation of breakwaters against tsunamis with long-duration overtopping using a large circulation pump; wave-induced seabed liquefaction using a wave generator; and sediment gravity flows in a large spatial domain in a drum container. For each case, the experimental approach and principal results are outlined.

## 2 EXPERIMENTAL METHODS USING DRUM CENTRIFUGE

A cylindrical container inside the drum centrifuge apparatus (manufactured by Broadbent, UK; installed and operated by Toyo Construction, Japan) is shown in Figure 2, together with an exterior view of the apparatus. The container has a diameter of 2.2 m, a width of 0.3 m, and a height of 0.3 m. The cylindrical container serves as a water flume and is filled with water. By installing wave or tsunami generators, or other equipment inside the drum flume, various hydraulic model experiments can be performed.

The generation and propagation of waves in a drum centrifuge were first studied by Sekiguchi and Phillips (1991). Baba et al. (2002) developed a wave generation system for a drum centrifuge based on a

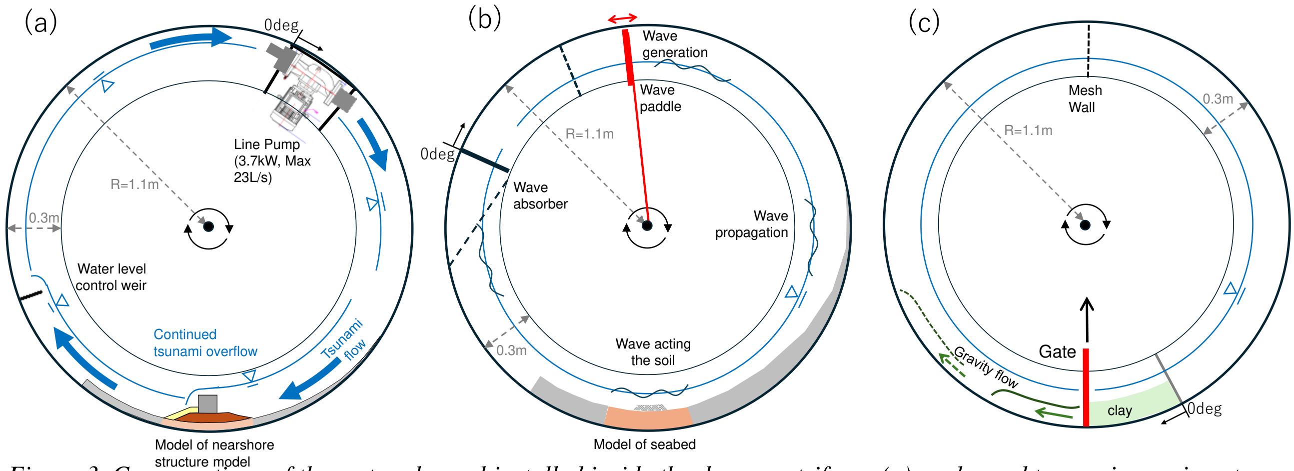


*Figure 3. Cross sections of the water channel installed inside the drum centrifuge: (a) prolonged tsunami experiment; (b) wave experiment; and (c) sediment gravity flow experiment.*

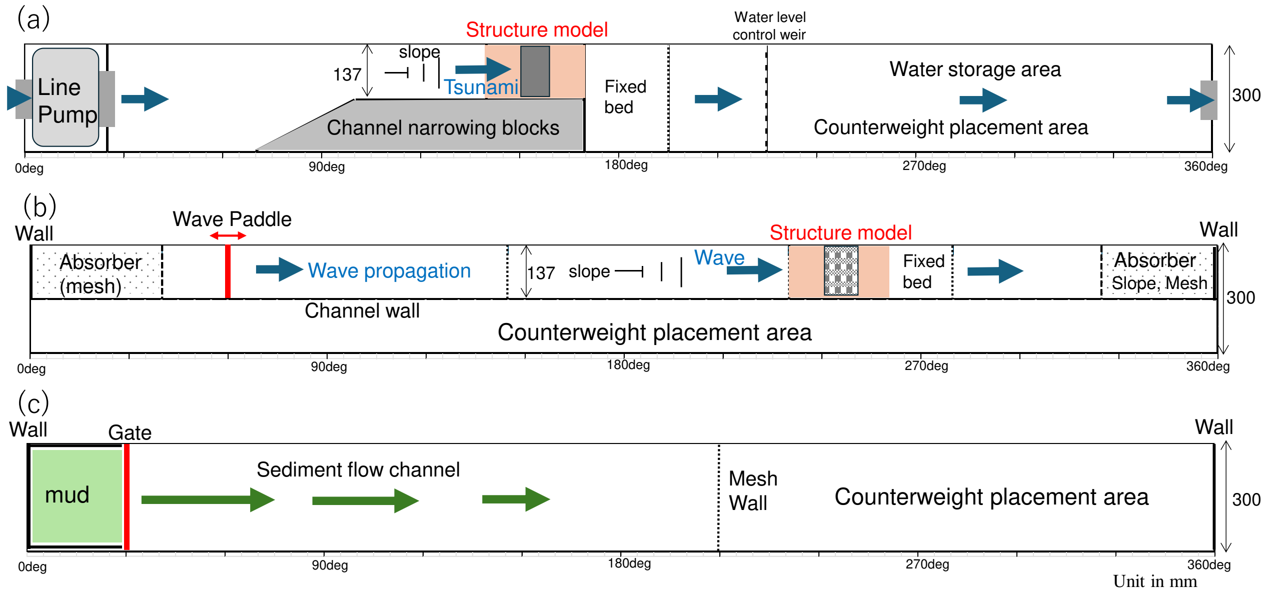


*Figure 4. Unwrapped top views of the water channel corresponding to Figure 3: (a) prolonged tsunami experiment; (b) wave experiment; and (c) sediment gravity flow experiment.*

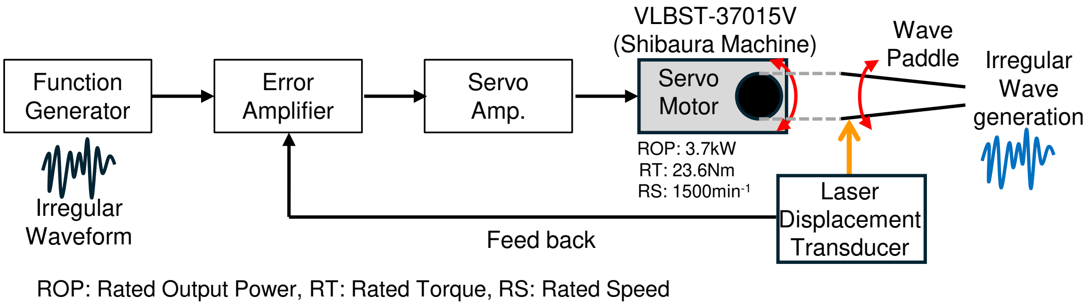


*Figure 5. System for generating variable amplitude and irregular waves in centrifuge wave experiments*

plunger-type device. Miyake et al. (2009) developed a bore-tsunami generation system using the dam-break method with a shutter gate. Tsurugasaki (2009) applied the dam-break method to centrifuge tests involving clay flow.

This paper illustrates three representative experimental methods developed for hydraulic centrifuge testing using a cylindrical container: tsunami experiments, wave experiments, and sediment gravity flow experiments. Figures 3 and 4 show cross-sections and unwrapped top views of the three corresponding water channels. The unwrapped top views are arranged in straight lines as seen from the centre of rotation.

Figure 3(a) shows the water flume for prolonged tsunami overflow experiments, enabling evaluation of resilient structures against large tsunamis. The flume is equipped with a large circulation pump (3.7 kW, maximum discharge 23 L/s). Its unwrapped top view is presented in Figure 4(a). Blocks are placed in the flume to reduce channel width and amplify tsunami height within the model area. The area behind the water level control weir serves as both a storage tank for sustaining constant tsunami flow and as a counterweight area to balance drum rotation.

Figure 3(b) shows the water flume for wave tests, featuring a wave paddle and a wave absorber. Its unwrapped top view is shown in Figure 4(b). The channel is divided into two zones: one for wave propagation and the other for counterweight placement, ensuring wave motion is not disturbed by the counterweight blocks. A distinct feature of this wave-test channel is that the wave paddle can be operated to generate specified waveforms, controlled by a feedback system consisting of an error amplifier and laser displacement transducer (LDT), as illustrated in Figure 5. To enable the wave paddle to perform reciprocal motion at a frequency of 10 Hz, a low-inertia servo motor (VLBST-37015V, manufactured by Shibaura Machine) was employed. This enables generation of waves with variable amplitude and irregular wave patterns.

Figure 3(c) presents the water flume designed for sediment gravity flow tests with a shutter gate. In this study, mud flow experiments are conducted, where the shutter is opened immediately after reaching the target centrifugal acceleration to prevent mud consolidation. Its unwrapped top view is shown in Figure 4(c). The channel is divided, with half dedicated to the flow area and the other half to the counterweight placement area.

# 3 OVERVIEW OF SCALING LAWS IN SOIL-WATER CENTRIFUGE EXPERIMENTS

## 3.1 Tsunami experiment: scaling law of seepage flow

Seepage flow is critical for the foundation stability of caisson-type breakwaters. Based on the Dupuit–Forchheimer equations, the hydraulic gradient in the rubble mound and sand bed is given by (Takahashi et al., 2014):

$$i = au + bu^2 \quad (1)$$

$$a = \alpha_0 \frac{\nu}{Ng} \frac{(1-n)^3}{n^2 D_{15}^2}, \qquad b = \beta_0 \frac{1}{Ng} \frac{1-n}{n^3 D_{15}} \quad (2)$$

where $u$ is seepage velocity, $\alpha_0$ and $\beta_0$ are cofficients, $\nu$ is dynamic viscosity of pore water, $n$ is mound or soil porosity, and $D_{15}$ is the 15 % grain size.

In sand beds, seepage flow is generally laminar and dominated by the first term of Equation (1). In contrast, rubble mound seepage is turbulent, dominated by the second term. Under centrifuge acceleration N$g$, to maintain similar seepage velocity,

In sand bed: $\nu_m = N\nu_p$ or $D_{15m} = N^{-0.5}D_{15p}$,

in gravel mound: $D_{15m} = N^{-1}D_{15p}$.

## 3.2 Wave tests: scaling law of pore pressure response

The development and dissipation of residual pore pressure $u_e$ under wave loading may be represented as follows (Sassa & Sekiguchi, 1999):

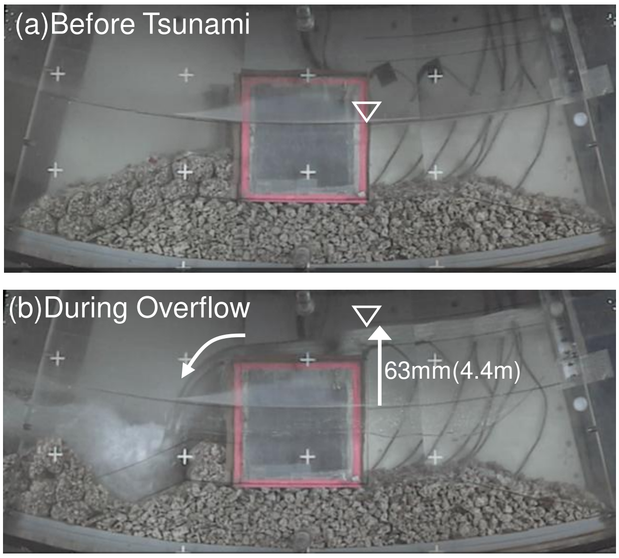


*Figure 6. Photographs of the caisson in the tsunami overflow experiment: (a) before the tsunami (C2-2 case); (b) during tsunami overflow (water level rise: 4.4 m).*

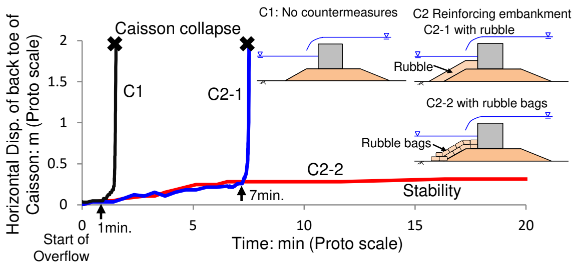


*Figure 7. Time histories of caisson displacement of tsunami overflow tests for three cases.*

$$\frac{\partial u_e}{\partial(\omega t)} = \frac{K}{m_v \nu \omega}\kappa^2 \frac{\partial^2 u_e}{\partial(\kappa z)^2} + \frac{1}{m_v}\frac{\partial \epsilon_{vol}}{\partial(\omega t)} \qquad (3)$$

where $K$ is the intrinsic permeability coefficient, $m_v$ is the coefficient of compressibility of the soil skeleton, $\nu$ is the dynamic viscosity of the pore fluid, $\omega$ is the angular frequency of waves, $\kappa$ is the wave number $2\pi/L$, $L$ is the wave length, $\varepsilon_{vol}$ is the plastic volumetric strain due to cyclic shearing, $z$ is vertical coordinate and $t$ is time. For consolidation time scaling, the following relationship must be satisfied for both model and prototype:

$$\frac{K}{m_v \nu \omega}\kappa^2 = const \qquad (4)$$

In a $1/N$ scaled model under acceleration $Ng$, $\kappa_m = N\kappa_p$, $\omega_m = N\omega_p$ following the Froude similitude. If the same soil and packing conditions are used, both $K$ and $m_v$ remain constant. Therefore, by setting $\nu_m = N\nu_p$, this relation is satisfied (viscous scaling; see Sassa & Sekiguchi, 1999, Miyamoto et al. 2019).

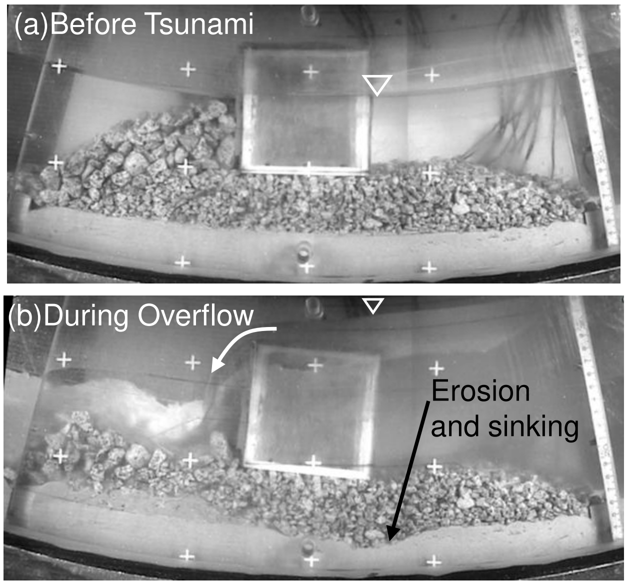


*Figure 8. Photographs of the breakwater placed on a sand bed: (a) before the tsunami ; (b) during tsunami overflow, showing sand erosion sinking the caisson.*

## 3.3 Gravity flow: scaling law of Reynolds number

We consider a subaqueous density flow of a viscous fluid (density $\rho_1$) in an ambient fluid (density $\rho_2$). The densimetric Froude number is $Fr_d = U/(g'H)^{0.5}$, and the Reynolds number is $Re = \rho_1 UH/\mu$, where $U$ is a representative velocity, $H$ the layer thickness, $\mu$: the apparent viscosity and $g' = g\,(\rho_1 - \rho_2)\,/\,\rho_1$ the reduced gravity. In a $1/N$ geometric scale under $Ng$ using the same material, $g'H$ is invariant; hence $Fr_d$ match between model and prototype.

For rheology, we adopt a Non-Newton Fluid (the Herschel-Bulkley model without the yield term): $\mu = K\dot{\gamma}^{n-1}$, with $0 < n \leq 0$, $\dot{\gamma}$ the strain rate, $K$ a cofficient. Since $\dot{\gamma} \sim U/L$, we have $\dot{\gamma_m} = N\dot{\gamma_p}$, so $\mu_m = N^{n-1}\mu_p$ and the Reynolds number scaling becomes $Re_m = N^{-n}Re_p$. Thus, while $n \rightarrow 0$ preserves $Re$, in practice $0 < n < 1$ makes the model $Re$ smaller by a factor between 1 and $1/N$. When the model and prototype flows are well within the high-$Re$ turbulent regime, this difference is usually negligible. Takahashi et al. (2020) applied the scaling with $n$=0 to fully liquefied sand flows.

It should be noted that the above scaling law applies only to fully liquefied (fluidized) flows. The characteristics of sediment flow strongly depend on excess pore-water pressure. As it dissipates, the sediment flow transitions from fluid-like to solid-like, resulting in significant changes in viscosity and flow regime. In this paper, we present clay-slurry flow experiments in which consolidation was negligible

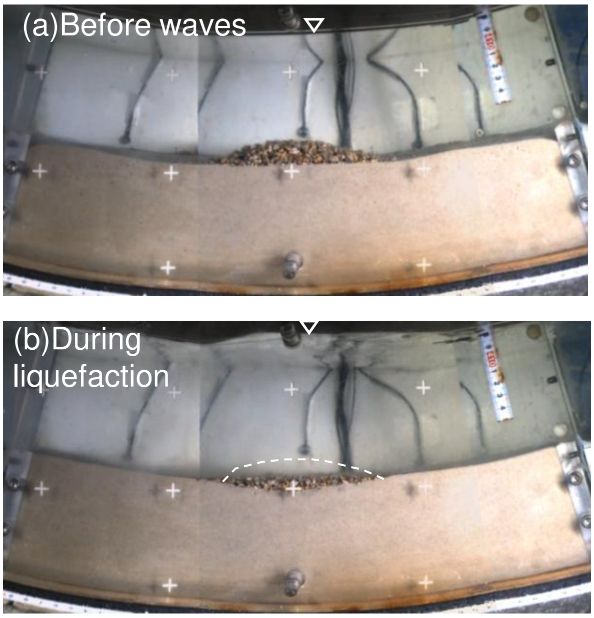


*Figure 9. Photographs of a submerged rubble mound placed on a loose sand bed: (a) before wave loading ; (b) during wave-induced liquefaction and significant sinking of the mound.*

over the very short flow duration, even in the centrifuge.

## 4 REPRESENTATIVE EXPERIMENTS AND RESULTS

### 4.1 Tsunami overflow tests and assessment of resilient structures

In this section, the resilience of breakwater against long-duration tsunami overflow was assessed using the experimental setup depicted in Figures 3(a) and 4(a). Three test cases were conducted under a centrifuge acceleration of 70 *g* (see schematic illustrations in Figure 7): C1) no countermeasures; C2-1) reinforcement with rubble; and C2-2) reinforcement with rubble bags. Figure 6 shows photographs of the breakwater with caisson before tsunami (C2-2 case) and during tsunami overflow. The tsunami caused a 4.4 m rise in water level in front of the caisson. The resilience of the breakwater against tsunami overflow was evaluated based on the displacement of the caisson (Figure 7). This figure shows the time histories of caisson displacement during overflow for each case. In C1, rapid movement and collapse of the caisson occurred after 1 minute of overflow in prototype time. In C2-1, significant movement and collapse were observed after 7 minutes. In C2-2, the caisson remained stable throughout the test period. In this case, overflow was sustained for over 40 minutes (34

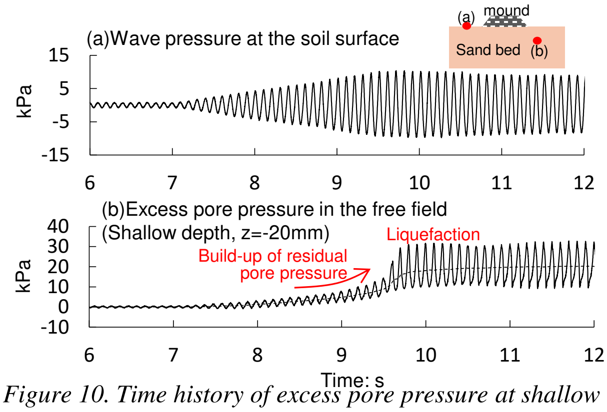


*Figure 10. Time history of excess pore pressure at shallow soil depth in the free field, together with input wave pressures.*

seconds in model time), which was limited by the data recording duration of high-speed camera.

Scour and erosion of the sand bed were also observed in a separate test case, in which a rubble mound was placed over a sand bed (Figure 8). The sand and rubble grain sizes were selected according to Eq. (2), in order to match the scaling laws of seepage flow velocity in both the sand bed and the rubble mound. During the tsunami overflow, sand transport through the mound was induced by seepage flow resulting from water level differences across the caisson.

### 4.2 Wave-induced liquefaction and sinking of a submerged gravel mound

This section demonstrates that a submerged rubble mound placed on a loose sand bed underwent significant sinking due to wave-induced liquefaction of the sand bed (Figure 9). The experimental setup used is depicted in Figures 3(b) and 4(b). The wave experiment was conducted under a centrifuge acceleration of 70 *g*. A pore fluid (Metolose) with a viscosity 70 times higher than that of water was used to achieve viscous scaling, as described in Section 3.2.

The time history of excess pore pressure at a shallow soil depth in the free field is shown in Figure 10, together with the input wave pressures. As the wave pressure on the soil surface increased, the residual pore pressure built up gradually, and reached the initial vertical effective stress level, indicating the occurrence of liquefaction at this depth. During wave loading, as the liquefied zone expanded both in depth and beneath the rubble mound, the mound significantly sank into the liquefied sand layer, as shown in Figure 9 (b) (Ito et al. 2020).

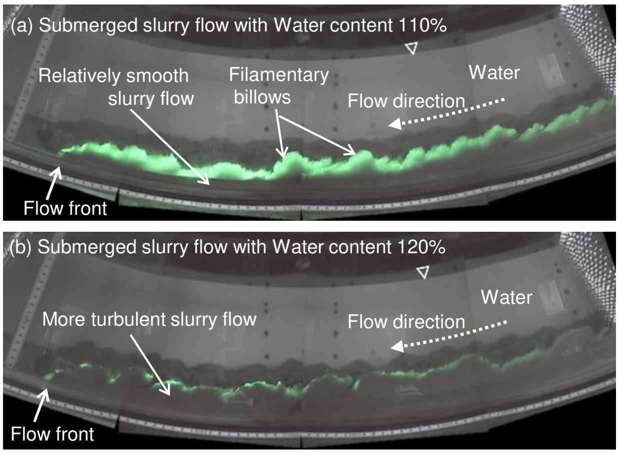


*Figure 11. Photographs of subaqueous gravity flows of clay slurry : (a) relatively smooth slurry flow (w=110%); (b) more turbulent slurry flow (w=120%).*

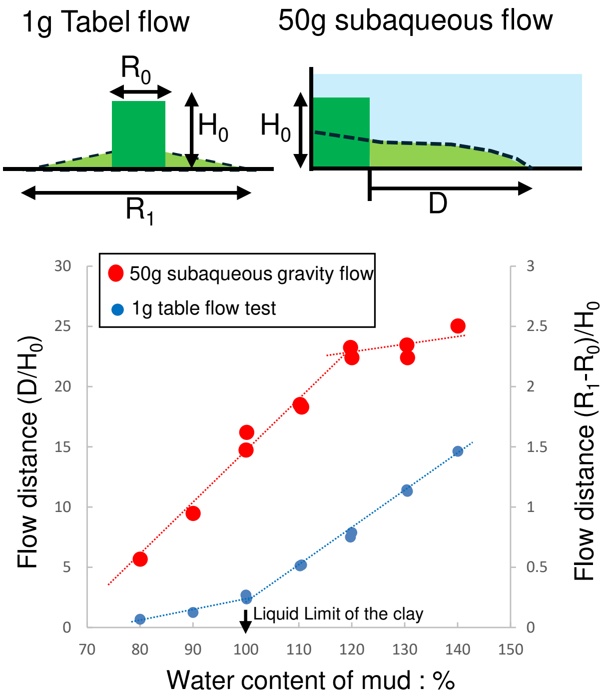


*Figure 12. Relationship between clay water content and flow distance at 50g and table flow tests at 1g.*

### 4.3 Subaqueous gravity flow of clay

This section presents observations of subaqueous clay flows under a centrifuge acceleration of 50 *g*. The experimental setup is shown in Figures 3(c) and 4(c). The water content of the clay was varied from 80 % to 140 %, where the liquid limit (LL) of the clay was 100 %. Two distinct flow patterns were observed (Figure 11). One was a relatively smooth flow accompanied by filamentary billows along the flow-water interface (Figure 11(a), at a water content of 110 %). The other was a more turbulent flow characterized by a thicker, diffuse mixing layer (Figure 11(b), at a water content of 120 %).

This change in flow pattern corresponds to the water content boundary of 120 %, as shown in Figure 12. The features of mud flow changed notably at this boundary. Figure 12 illustrates the relationship between water content and flow distance, together with the results of table flow tests conducted under 1*g*. For subaqueous gravity flows at 50 *g*, the flow distance increased with water content, but the rate of increase decreased at the water content boundary of 120 % (1.2 LL). In the 1g flow tests, the rate of increase in flow distance increased at the boundary of water content 100 % (1.0 LL). It can also be seen from this figure that the dimensionless flow distance of subaqueous gravity flows at 50 *g* is significantly greater than that of the table flow tests at 1*g*. These findings highlight the importance of evaluating submerged sediment flow under prototype stress fields.

## 5 SUMMARY

This paper demonstrates that drum-type centrifugal hydraulic model experiments are effective for examining wave–soil–structure interactions and system stability. Key offshore processes, such as tsunamis, high waves, and submarine sediment flows, are physically modelled using this approach. The principal findings of this paper may be summarized as follows:

(1) Three representative experimental methods developed for hydraulic centrifuge testing using a cylindrical container were illustrated: prolonged tsunami overflow experiments, wave experiments enabling generation of variable amplitude and irregular wave patterns; and sediment gravity flow experiments using the large spatial domain of the drum container.

(2) Scaling laws for representative water-soil experiments were presented based on the equations, focusing on seepage flow in rubble mound and underlying soil induced by tsunami, viscous scaling for pore pressure responses during wave loading and Reynolds number of viscous slurry flow.

(3) Representative experimental results of water-soil-structure interaction experiments using the drum centrifuge were presented: assessment of resilient structure of the breakwater against prolonged tsunami overflow, sinking of the submerged rubble mound in association with wave-induced liquefaction and progress of liquefaction, and effects of water content of clay on flow distance and the importance of

evaluating submerged sediment flows under prototype stress fields.

## REFERENCES


Baba, S, Miyake, M., Tsurugasaki, K. and Kim, H. (2002). Development of wave generation system in a drum centrifuge, Proceedings of the ICPMG ‘02, St. John’s, Newfoundland, Canada, pp. 265-270. https://doi.org/10.1201/9780203743362

Ito, H., Miyamoto, J., Sassa, S. and Sumida, H. (2021). Drum centrifuge tests on wave-induced liquefaction and sinking of submerged rubble mound, Journal of Japan Society of Civil Engineers, Series B3 (Ocean Engineering) , 77-2, pp. I_511-I_516. 10.2208/jscejoe.77.2_i_511 (in Japanese)

Miyake, M., Sumida, H., Sakai, H. and Imase, T. (2009). Development of centrifuge modelling for tsunami and its application to stability of a caisson type breakwater, Annu. J. Civil Eng. Ocean, 25, pp. 87-92. (in Japanese)

Miyamoto, J., Sassa, S., Tsurugasaki, K. and Sumida, H. (2019) . Wave-Induced Liquefaction and Floatation of a Pipeline in a Drum Centrifuge, Journal of Waterway, Port, Coastal, and Ocean Engineering, ASCE, Vol. 146, Issue 2, 04019039. https://doi.org/10.1061/(ASCE)WW.1943-5460.0000547

Sassa, S. and Sekiguchi, H. (1999). Wave-induced liquefaction of beds of sand in a centrifuge, Géotechnique, 49 (5), pp. 621-638. https://doi.org/10.1680/geot.1999.49.5.621

Sekiguchi, H. and Phillips, R. (1991). Generation of water waves in a drum centrifuge, Centrifuge 91, pp. 343-350.

Takahashi, H., Sassa, S., Morikawa, Y., Takano, D., and Maruyama, K. (2014). Stability of caisson-type breakwater foundation under tsunami-induced seepage, Soils and Foundations, 54 (4), pp. 789-805. https://doi.org/10.1016/j.sandf.2014.07.0024

Takahashi, H., Sassa, S. and Fujii, N. (2020). Centrifuge model tests of earthquake-induced submarine landslide, Inter-national Journal of Physical Modelling in Geotechnics, 20(4), pp. 254-266. https://doi.org/10.1680/jphmg.18.00048

Takahashi, H., Zdravkovic, L., Tsiampousi, A. and Mori, N. (2024). Destabilisation of seawall ground by ocean waves, Géotechnique, 74 (8), pp. 713-728. https://doi.org/10.1680/jgeot.21.00420

Tsurugasaki, K. (2009). Development of a drum-type centrifuge model testing method and its application to real coastal problems, Doctoral dissertation, Kyoto University. https://doi.org/10.14989/doctor.k14591 (in Japanese)

Tsurugasaki, K., Miyamoto, J., Hem, R., Iwamoto, T. and Nakase, H. (2018). Centrifuge model tests on stabilization countermeasures of a composite breakwater under tsunami actions. Proceedings of ICPMG 2018. pp. 675-680. https://doi.org/10.1201/9780429438660